Available online at www.qu.edu.iq/journalcm
JOURNAL OF AL-QADISIYAH FOR COMPUTER SCIENCE AND MATHEMATICS
ISSN:2521-3504(online) ISSN:2074-0204(print)

Iris Recognition in Cross-Spectral Based on Histogram of Oriented Gradient and Linear Discriminant Analysis

Nisreen Mzehir AL-kardhi[1] , Ali Mohsin Al-juboori[2]

[1]College of Computer Science and Information Technology, Al-Qadisiyah University, Iraq. com21.post11@qu.edu.iq

[2]College of Computer Science and Information Technology, Al-Qadisiyah University, Iraq: Ali.mohsin@qu.edu.iq

ARTICLE INFO

Article history:
Received: 25 /05/2023
Rrevised form: 25 /07/2023
Accepted : 01 /08/2023
Available online: 30 /09/2023

Keywords:

Iris Recognition, Cross-spectral matching, HOG, LDA, KNN, SVM

ABSTRACT

The use of biological and behavioural characteristics has significantly increased in recent years. Like fingerprints, faces, iris, and others in numerous crucial applications in security and electronic governance. Where recently, Research has concentrated on illuminating the recognition of iris images obtained in different fields across spectra by sensors that can capture double iris images in various areas (environment/lighting) by infrared Nearby and visible illumination (NIR, VIS) due to features unique in the iris texture that differ for the same individual, between their left and right eyes. But there is challenging to match NIR and VIS photographs due to the spectrum differences between pictures captured by near-infrared and visible light. We suggest utilizing the Histogram of Oriented Gradient (HOG) approach to extract meaningful information from images of the iris and implement Normalization to reduce differences in illumination, also apply the LDA for dimensionality reduction and K-Nearest Neighbor and Support Vector Machine as a classifier. The experimental findings were implemented on the PolyU bi-spectral dataset, and the results show that the suggested approach achieved exceptional matching performance by KNN, SVM on (Right to Left) for each (NIR, VIS) or versa (99.14%,99.04%, 97.44%,96.38%) respectively.

MSC.

https://doi.org/10.29304/jqcm.2023.15.3.1267

1. Introduction

Iris biometric systems play a significant part in identifying a person. Compared to other biometrics, it relies on the unique precise details of characteristics in iris texture that are thought to be established randomly throughout the eye's embryonic development, also considered to differ across individuals in both the left and right eyes of the same. The appearance of the iris remains stable mainly for most of a human's life.[1]. However, there are considerable challenges when comparing iris pictures taken in

∗Corresponding author

Email addresses:

Communicated by 'sub etitor'

several spectral bands, such as VIS at 400-750 nm and NIR at 750-1400 nm. As a result, it is more challenging when performing matching between iris images in the NIR and VIS spectrums than it is to do so in the same domain [2].

Because The reflection that occasionally obscures the iris pattern has a substantial impact on recognition ability, also, using NIR images iris recognition is more successful in identifying persons than VIS images because there are fewer reflections in NIR iris images than in VIS images[3]. as shown in Figure (1). The distinctive textural pattern seen in the iris may be extracted using various feature extraction techniques, and the pattern can also be saved as a template.[4]

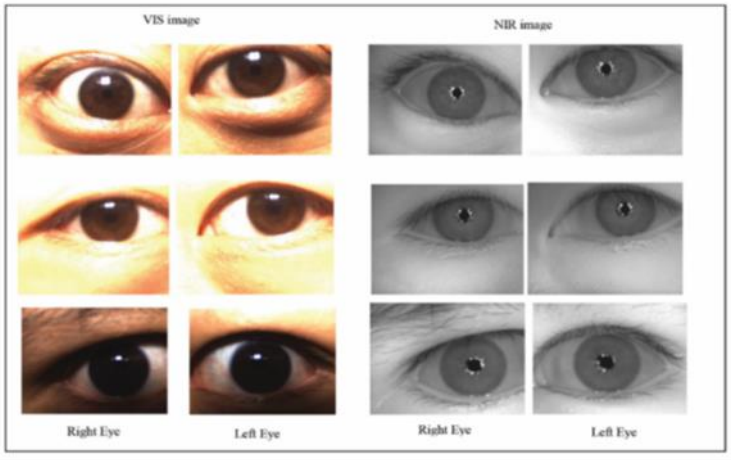

Fig 1: shows the human eye iris in the cross-spectral domain (image source:polyU database in [5])

The present study also focuses on cross-spectral NIR-VIS recognition, how to minimize the high dimensionality of iris codes, and how to lessen the impact of these aspects that affect overall performance and recognition accuracy, .where feature extraction techniques frequently produce high-dimensional. This causes considerable complexity and places a heavier computing burden on the classifier, degrading classification performance. This study employed DCT_normation used as photometric normalizing based discrete cosine transform (DCT) filtering, a Histogram of Oriented Gradient (HOG) as a feature extraction approach, followed by adding LDA as a feature selection strategy and representing the iris sample with lower dimensionality. We also categorized iris patterns using KNN and SVM.

This study was already done in iris identification in cross-spectral was reviewed in Section 2, where recommended methodologies were presented in Section 3 and Conclusions and recommendations for further research are offered in Section 5 after the recommended approaches have been reviewed and evaluated in Section 4

2. Related Work

This section will focus on a review of recent studies that summarize that iris recognition was the most accurate due to its high accuracy and distinctive texture patterns in iris images, with significant challenges when matching iris images obtained from different domains. It will also cover several deep learning and machine learning techniques for iris-based recognition systems.

Whereas Kuo Wang et al. [6] proposed cross-spectral iris recognition using developed a deep learning architecture for cross-spectral iris detection that includes convolution neural networks (CNNs) with softmax cross-entropy loss and supervised discrete hashing throughout the training process (SDH). Because SDH reduced the template matching database size, the experiment's results demonstrate higher performance accuracy in high cross-spectral iris image matching speed. Experiment models suggested on the PolyU bi-spectral dataset for 140 subjects were applied style self-learned and SDH for compression classification. Achieve advanced results is 90.71%also the equal error rate (EER) is 5.39%.

While Maulisa Oktiana et al. [7] used a photometric normalization method using homomorphic filtering and phase-based cross-spectral iris detection. This study provided a phase-based way. The 2D (DFT) phase component of the (NIR, VIS) iris images was used to determine the matching score. Where used PLPOC. A recently developed method has excellent performance, is easy to use, and requires 0.59% of the computational resources. While obtaining the phase correlation between (NIR, VIS)iris images can be complex, homomorphic filtering outperforms other methods in lowering specular reflection, utilizing the iris database at PolyU: 0.59% EER and 95%.

Moktari Mostofa et al .[8]proposed a new study based on a convolutional generative adversarial network design that operated on two different principles, either on the conditional (cGAN), or a coupled generative (cpGAN) techniques to reduce the distance between (VIS, NIR) Identical person's iris, The goal of it is to improve accuracy and correlation by using cross-spectral iris identification. By practising joint translation high-resolution methodology, both methods match cross-spectral iris inside the same domain with the exact resolution. The experimental (CpGAN) on (High Resolution of VIS) versus (High Resolution -NIR) is 92.38% yielded successful results across the latent embedding subspace.

Another research Ritesh Vyas et al. [9] for extracting iris features that require splitting the iris image into blocks and then calculating variances for the partitioned image's sub-blocks to retrieve the iris's textural properties at various frequencies and angles and difference of conflicts (DOV) for characteristics that are noise-free globally brought on via changes in illumination, location employs a Gabor filter bank. To filter the iris template, the results show that the suggested technique outperforms when applied on IITD and PolyU databases in terms of performance. The method is relatively easy because it needs to know the actual mean and standard deviation formulas. With the IITD database, the best GAR value is 98.3%, while the best cross-spectral (VWNIR) matching value is 68.98.

A novel strategy described by Maulisa Oktiana et al. [10]. Due to the difficulties in separating the iris from pictures taken with the VIS and the NIR spectrum, there are variations in illumination factor and an EER of greater than 5%. In the normalization phase, this paper presents a new technique (GRF) based on Integrated Gradient face-Based Normalization, in which GRF is computed for each pixel in the normalized form of the iris picture and how it depicts the relation among pixels. The results of the experiments showed improved cross-spectral iris identification ability in matching, with lowered EER of 1.02 at GAR 98.97.when the Gabor filter is used with the Poly U iris database (GRF, BSIF, and DOG).

They suggested Maulisa Oktiana et al. [11], A method based on Multi-Scale Weberface (MSW) cross-spectral for iris matching, which combines Gabor with Local Binary Pattern (GLBP) integration with MSW. They also used the CHT technique to divide both (VIS and NIR) iris images. After that, the images are normalized using Daugman rubber sheet normalization and one of the photometric normalizing methods, MSW, which compares the local intensity variation and its sensitivity to changes in the illumination sources. Experimental results demonstrate that the new method is more accurate. Where show that MGLBP has a more significant recognition rate under different reference criteria by 9%, and the recognition rate increases by 40% when employing MGLBP on PolyU iris because MGLBP can

effectively extract the prominent pattern from the iris image. It achieves a greater recognition rate than LBP and GLBP.

All studies assessed the capability of cross-spectral iris identification to improve matching accuracy. Several of them struggle with normalization challenges. Research on feature selection and dimensionality reduction is vital for developing efficient regression and classification models to support decision-making using data-based learning strategies.

Table 1:Summary of Related Work

Ref	Proposed techniques	Year	Subject	Dataset	Accuracy
[15]	MSW, MGLBP	2018	150 subject	PolyU database	100 %
[14]	DOV,2DGaborfilter bank	2018	70 subject (1050 images)	PolyU database	68.98%
[12]	GRF, BSIF, DOG	2019	75 subject	PolyU database	98.97%
[24]	CNN, SDH	2019	140 subject 209 subject	PolyU database	90.71% on(140) 64.67% on (209)
[22]	PLPOC, 2D- DFT	2020	209 subject (12000) image	PolyU dataset	95%
[35]	CpGAN	2020	209 subject	PolyU database	92.38%,

3. Proposed Method

The suggested model for cross-spectral iris identification has been tested on (VIS and NIR) iris pictures. Due to varying lighting conditions, will need into the pre-processing process is necessary as an illumination normalization approach for iris images left and right (NIR, VIS), where illumination variations can be significantly reducedThen, separate both NIR and VIS images into four blocks—then applying a Histogram of Oriented Gradient for an extracted feature from each Block. Then, combine these feature blocks for the input picture, such as (NIR, VIS) and extracted elements (NIR and VIS), by also combining features NIR and VIS to create final feature vectors (VIS+NIR), after which apply LDA. Applying Linear Discriminant Analysis as a technique for dimensionality reduction and feature selection might result in results that are even more accurate than those obtained solely by classification techniques. Next,

partition the feature dataset into testing and training templates using this process's findings. Apply KNN and SVM as a classifier, and then finish. As Fig 2

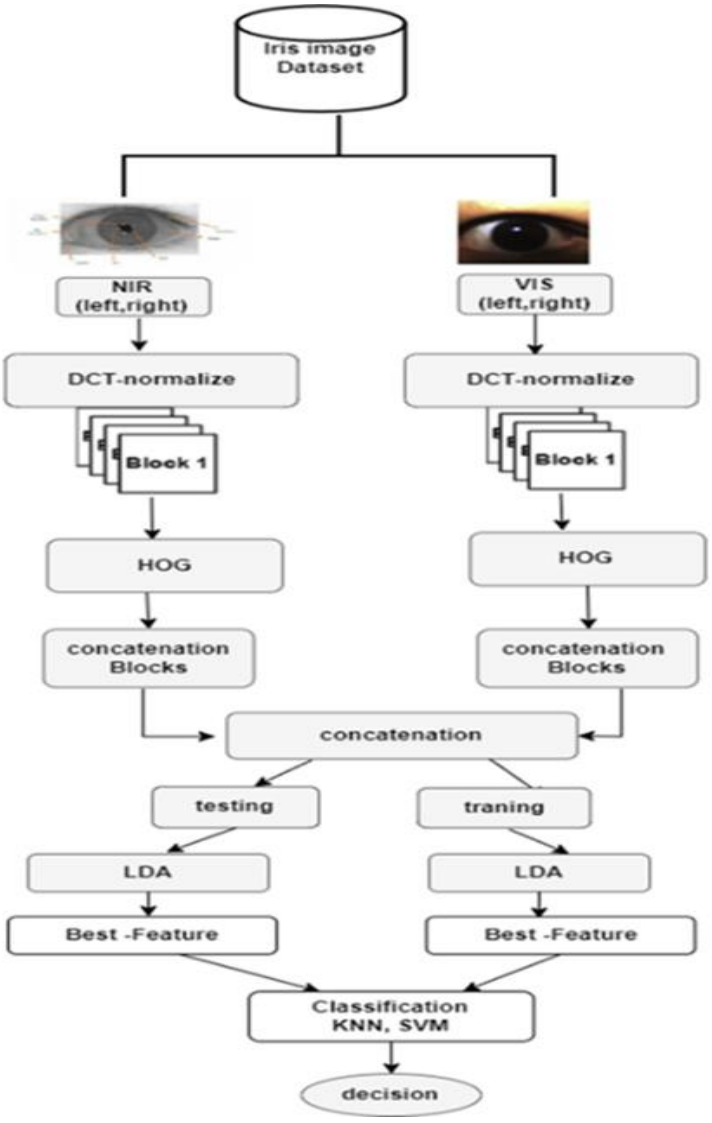

Fig 2: shown Proposed Model

3.1 Normalization Technique-Based DCT

To perform photometric Normalization of the image. An image can be converted from the spatial domain to the frequency domain using the commonly used orthogonal transform known as the discrete cosine transform (DCT) coefficients technique to remove some of the low-frequency information in the images. [12]. a suitable number of DCT coefficients are truncated for low-frequency DCT coefficients are applied after converting images into the Logarithm transform domain—the definitions of DCT and the inverse transform.

The descriptions of DCT and the inverse transform are as follows.[13].

$$D(p1,q1) = \varepsilon(p1)\varepsilon(q1)\sum_{u=0}^{U-1}\sum_{v=0}^{V-1} G(u,v) \times cos\left[\frac{\pi(2u+1)p1}{2U}\right] cos\left[\frac{\pi(2v+1)q1}{2V}\right] \quad (1)$$

where p1=0, 1, 2, 3,..., U - 1 and q1=0, 1, 2, 3,..., V - 1 respectively.

Also, it is possible to define the inverse discrete cosine transform (IDCT) as

$$G(u,v) = \sum_{u=0}^{U-1}\sum_{v=0}^{V-1} \varepsilon(p1)\varepsilon(q1)\ D(p1,q1) \sum_{u=0}^{U-1}\sum_{v=0}^{V-1} \times cos\left[\frac{\pi(2u+1)p1}{2U}\right] * \ cos\left[\frac{\pi(2v+1)q1}{2V}\right] \quad (2)$$

$$(p1) = \begin{cases} \frac{1}{\sqrt{U}} & p1 = 0 \\ \sqrt{\frac{2}{U}} & p1 = \ 0, 1, 2, 3, \dots, U - 1 \end{cases} \quad (3)$$

$$\varepsilon(q1) = \begin{cases} \frac{1}{\sqrt{V}} & q1 = 0 \\ \sqrt{\frac{2}{V}} & q1 = \ 0, 1, 2, 3, \dots, V - 1 \end{cases} \quad (4)$$

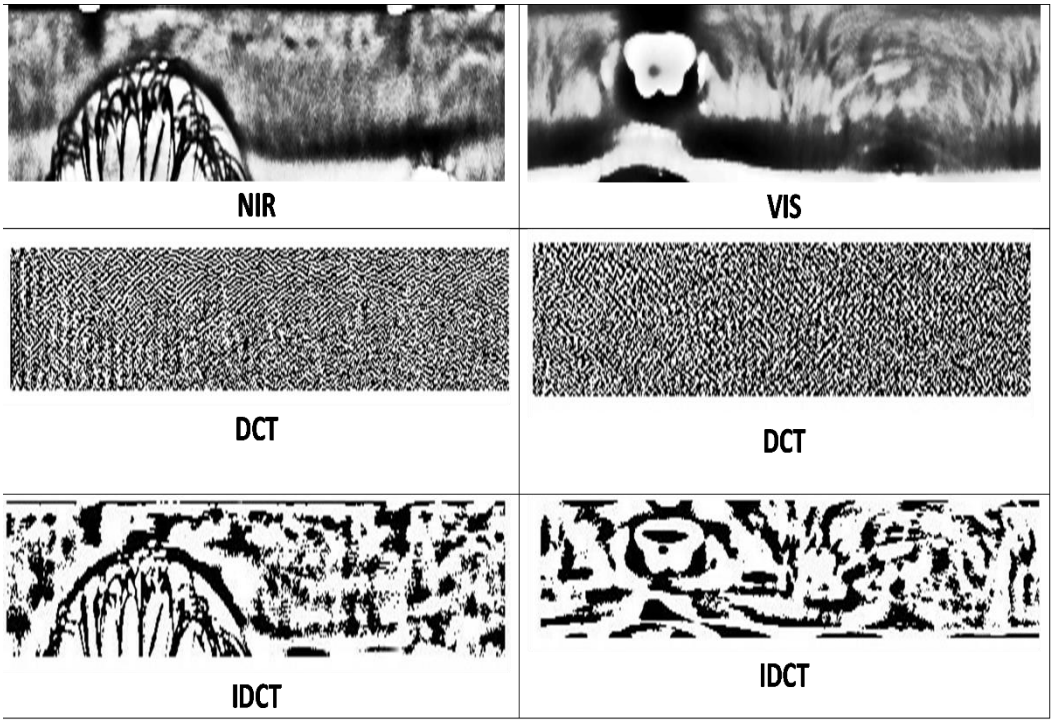

Fig 3:Shows apply a discrete cosine transform and inverse discrete cosine transform on sample the (NIR, VIS)

3.2 Histogram of Oriented Gradients

HOG refers to a directed gradient histogram, whose essential component is statistical gradient data. Due to their great descriptive power, resistance to variations in illumination, simplicity, and ease of implementation, the methods developed by N. Dalal and B. Triggs have been widely utilized in various computer vision applications, including face recognition and vehicle identification. [14] The distribution of local intensity gradients or edge orientations can commonly accurately depict the appearance and shape of nearby objects even when the related gradient or edge coordinates are unknown. [15]. The input image will be partitioned into tiny spatial sections (cells), with each cell collecting a local 1-D histogram of edge orientations or gradient directions across its pixels. We generated local histograms of a gradient following the methods below to get a comprehensive descriptor of the image, as in

Fig 4: Shows a diagram of HOG feature extraction (image source:[16]).

A picture has easily been generated by filtering Gaussian 8x8 with a sigma=0.5 was used for the orientations between 0 and 90 to compute the gradient images for both the horizontal and vertical. The way of its implementation is to obtain the gradient component in the X and Y directions, as well as the pixels (x,y) from the original image, respectively. Then, by applying formulae (5) and (6), it is possible to compute the horizontal gradient and vertical gradient at each input image pixel [15]

$$G_x(x,y) = P(x+1,y) - P(x-1,y) \quad (5)$$

$$G_y(x,y) = P(x,y+1) - P(x,y-1) \quad (6)$$

G_x (x,y) When the horizontal gradient is x, in (x, y), G_y (x,y), In (x, y), y represents the vertical gradient., and P (x, y) is the pixel value at (x, y) in the formula above. Thus, the gradient direction at pixel (x,y), as well as the gradient amplitude G(x,y) may be shown to be as follows: [14].

$$G(x,y) = \sqrt{G_x(x,y)^2 + G_y(x,y)^2} \quad (7)$$

$$\theta(x,y) = tan^{-1}\left(\frac{G_y(x,y)}{G_x(x,y)}\right) \quad (8)$$

For each cell, we create an oriented gradient histogram. Constructing the directed gradient histogram for each cell Cells are 8x8 pixels in size. We calculate the gradient histogram for each cell based on bins 9 for each direction. L2-No normalizes each Block of cells' histograms before being concatenated to create the Block's final HOG feature.

The Number of features for each Block is 3,348 features. The Total Number of components extracted from the image is 13,392. Fig 5 displays the result when applying HOG on images of both VIS and NIR.

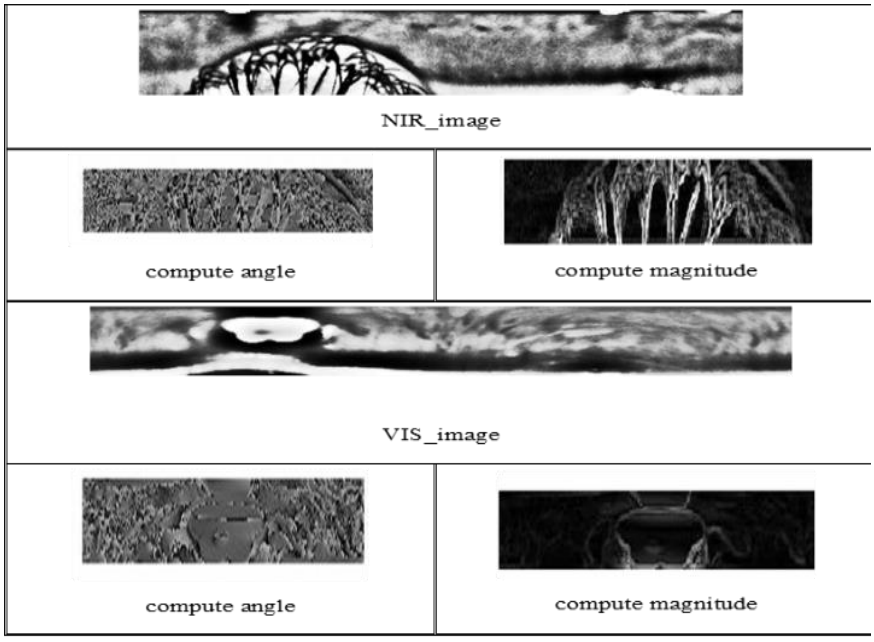

Fig 5:Show to use the (HOG) on the Left and Right (NIR, VIS)

3.3 Linear Discriminant Analysis

LDA was developed by Fisher in 1936.LDA was used as a feature reduction method due to the Dataset containing redundant and irrelevant data. This will affect the accuracy of the classifier, where the primary goal is to minimize this ratio within the class while increasing the distance between types. as shown in the following[17]

$$Z = W^T y \quad (9)$$

When employing a transformation matrix technique, this strategy was utilized for data with high dimensions create low-dimensional of data and computed as Where $\boldsymbol{y} \in \boldsymbol{U^d}$ high-dimensional original information, $\boldsymbol{W} \in \boldsymbol{U^{d\times m}}$ transformation matrix (d >n). $\boldsymbol{Z} \in \boldsymbol{U^m}$ The low-dimensional data obtained after transformation is the low-dimensional data obtained after transformation.

LDA's core principle is that points belonging to the same class should be as close as practical, while attributes belonging to different kinds should be as far away, $\boldsymbol{S_W}$ represents the within-class scatter matrix, a $\boldsymbol{S_B}$scatter matrix between classes $\boldsymbol{S_{to}}$ Scatter matrices for all classes are as follows[19]

$$S_W = \sum_{k=1}^{K} \sum_{i=1}^{M} X_{k_i} (y_i - \mu_k)(y_i - \mu_k)^T \quad (10)$$

$$S_B = \sum_{k=1}^{K} (\sum_{i=1}^{M} X_{k_i})(\mu_k - \mu)(\mu_k - \mu)^T \quad (11)$$

$$S_{to} = \sum_{k=1}^{K} \sum_{i=1}^{M} X_{k_i} (y_i - \mu)(y_i - \mu)^T \quad (12)$$

Where μ_k mean vector of class k

$$\mu_k = \frac{1}{M_k} \sum_{i=1}^{M} X_{k_i} y_i \quad (13)$$

$$M_k = \sum_{i=1}^{M} X_{k_i} \quad (14)$$

is the class k cardinality. The calculation for the total mean vector **μ** is

$$\mu = \frac{1}{M} \sum_{i=1}^{M} y_i \quad (15)$$

.

Where The class k cardinality is represented by the class k mean vector μ_k .The calculation for the total mean vector **μ** is,$Y \in \{y_i \in U^d | i = 1,2, \dots, m\} \in U^{d \times m}$, be the training set of data, where d represents the input samples' dimension, and There are m samples. The samples are divided into K classes and also every data y_i is equivalent to the class label k.($1 \leq k \leq K$). K stands for the dataset for class k and M_k, is the data points for class k. Notation μ_k: is the mean of the class k data points, and μ is the data's overall average points. (.)stands for the transposition of the matrix. The conventional LDA handles this issue..[20]

$$W_{opt} = argmax_W tra \left[\frac{W^T S_B W}{W^T W_S W} \right] \quad (1)$$

Where tra is the matrix's trace.. The most effective projection matrix .W is possible by calculating the eigenvectors of $W = {S_W}^{-1} S_B$ being in accordance with the first m greatest

3.4 Classification

Establishing a separate category based on training data is the aim of categorization. A classifier is needed to forecast class labels and verify the model utilized in this study, which is expected to produce reliable results (K-NN) (SVM).

3.4.1 K-nearest neighbour(KNN)

one of the most fundamental algorithms for machine learning that classify unknown data using training datasets that have already been recorded is The distance between the training dataset and the novel or testing dataset[21]is calculated using a similarity metric such as the Euclidean distance, cosine similarity, or the Manhattan distance. This algorithm for calculating the distance between data conducts a hypothetical investigation to ensure that the data close together are similar and far apart from others. It doesn't have to know how to execute complicated mathematical computations. Utilizing the equation [22], one may compute. This Research was used. The variable k represents the Number of neighbours,

$$d(x,y) = \sqrt{\sum_{i=1}^{n}(x_i - y_i)^2} \qquad (18)$$

Where: d (x,y) are Two points in Euclidean distance,x_i, y_i Are Euclidean Vectors, n is n-space.

3.4.2 Support vector machine classifier (SVM)

SVM analyzes the results of the classification and regression analysis. SVM is a supervised learning model with an associated learning method.[23] The critical idea in SVM is the concept of kernel function. Handling situations where the data are not linearly separable involves translating the data space entries into a space with a more significant dimension called feature space[24]. In this paper, we choose kernel functions. Polynomial kernel: are:

$$K(a_i, b_i) = \left(\gamma a_i . a_j + r\right)^{d} \ , \gamma > 0 \qquad (19)$$

Where a_i, b_i Corresponding to two separate observations in the Dataset, r determines the polynomial coefficient, d is the degree of the polynomial and γ the parameters that control the polynomial's effect are traded.

4. Results and Discussion

In this part, we first provide the datasets and training information to demonstrate the use of our technique. We contrast our method's performance with other cross-spectral iris identification techniques already used to illustrate its effectiveness for cross-domain iris recognition.

4.1 Dataset

Database for PolyU bi-spectral data from The Hong Kong Polytechnic University was made accessible to the public using the suggested models. The Dataset contains 418 classes of iris pictures in Bi-spectral taken from (209 people), and where database comprises iris pictures obtained using dual-eye (right and left) simultaneous bi-spectral imaging. Additionally, Each spectrum has 15 instances in each class. There there are a total of 12540 iris photos (209×2 ×2 ×15). Where 640 x 480 pixels is the size of the origin photos, this publicly available implementation iris segmentation algorithm for separating iris pictures from eye images. Additionally, offer an automatically segmented (512 x 64) pixel picture of the iris. Displays some photos from the database.[26]

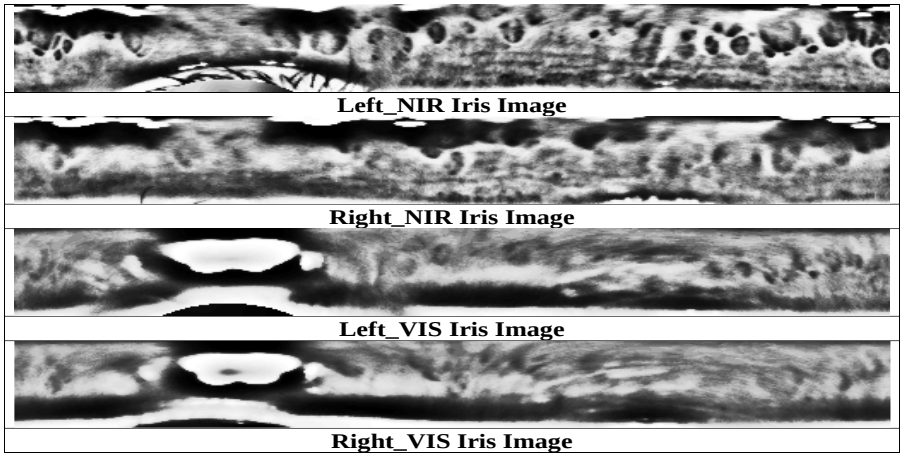

Fig 6: show the left and right of the iris image of a person in the cross-spectral domain

4.2 Model Performance Evaluation

The accuracy of the computation is used to evaluate performance. The model's accuracy measures how frequently it is correct[25]

$$accuracy = \frac{TP + TN}{TP + TN + FN + FN} \qquad (20)$$

TP: True positive, TN: True negative, FP: False positive, FN: False negative

Table 1:Comparative Result Analysis of Proposed Technique with HOG+LDA with (KNN, SVM)

Ref	Year	subject	Accuracy
Kuo Wang [6]	2019	140 subject 209 subject	90.71% 64.67%
Maulisa Oktiana [7]	2020	209 subject	95%. On 209 s
Moktari Mostofa[8]	2021	209 subject	92.38%
Left NIR vs RightVIS **Right NIR vs LeftVIS**	-	209subject	In KNN (99.14%,99.04%) In svm (97.44%,96.38%)

As shown in Table (1), our suggested HOG and LDA-based method succeeds in cross-spectral domain recognition to get the best results on the poly U bi-spectral dataset.

When trials were conducted on 209 subjects using KNN classifier on iris images in which, the cross-spectral accuracy rates for (left-NIR vs right-VIS) and (right-NIR vs left-VIS) were 99.14 and 99.04%, respectively,

when performing experiments by applied Support Vector Machine (SVM) as classifier has resulted. The experiment implements an iris accuracy rate on 209 subjects using iris images. The cross-spectral accuracy rates for (left-NIR vs right-VIS) and (right-NIR vs left-VIS) were and97.44% and 96.38 respectively.

These experiments also used LDA to reduce dimensionality and achieve a low mistake rate while increasing accuracy. This paper implements an investigation on 209 subjects, while most papers display other approaches reported in the literature applied on the part of subjects.

While Kuo Wang [6] created the author's cross-spectral iris recognition technique in 2019 based on CNN and Supervised Discrete Hashing with softmax cross-entropy loss of 90.71% (FAR = 0.01) when applied to 140 subjects and 64.67% (FAR = 0.01) when applied to 209 subjects.

While the author's cross-spectral iris recognition method developed by Maulisa Oktiana [7] in 2020 based on a phase-based matching approach uses homomorphic filtering, as well as 2D-DFT for extract feature, was experimental results applied on 209 subjects in 95%, while the author'sMoktari Mostofa in [8] 2020 applied to compare between NIR-VIS used based on two different GAN-based frameworks based cross-spectral iris recognition was accuracy rate 92.38% on 209 subjects. We divided the Dataset for the experiment into 70% training and 30% as testing sets, respectively. A fixed computer equipped with an i7-1165 processor, 8 Gb of RAM, and an Intel 2.5 CPU has been used for experiments.

5. Conclusion

This paper discusses how iris recognition, where the article' on strategies investigated with various methods focuses on four crucial phases, Normalization, feature extraction, selection feature and classification, and the Algorithm utilized to get results accuracy. Because the information important in iris texture is important and relevant in information security, iris recognition systems have recently been widely employed in various applications because it is unique, reliable over time, and well-protected.

The proposed method proved effective in person identification based on iris images acquired from different domains. This framework produced successful outcomes on the poly U Bi-spectral dataset using the suggested (HOG+LDA) model. From the comparative results, Also, LDA succeeded in reducing the number of features and removing unnecessary elements and also succeeded in DCT_nomalization in reducing the spectral gap between iris images. Because most datasets contain noise and undesired regions, pre-processing the Dataset before feature extraction, such as picture improvement and cropping, is particularly significant and enhances accuracy. It was found that the proposed method achieved higher accuracy than the models presented in previous works.

Future research will examine alternative methods for enhancing recognition performance by automatically producing the iris region obscured by reflected light, eyelash, eyelid, and glasses frame, as well as how examined for reducing the errors of simple matching or imposter matching caused by the dependence on the periocular region when the eyelid shape is changed due to off-angle or a change in facial expression ., and how to combine these algorithms with the internet of things to achieve complete automation from data collection to processing.

References

[1] G. Gautam and S. Mukhopadhyay, “Challenges, taxonomy and techniques of iris localization : A survey,” Digit. Signal Process., vol. 1, p. 102852, 2020, doi: 10.1016/j.dsp.2020.102852.
[2] A. Adekunle et al., “Feature Extraction Techniques for Iris Recognition System: A Survey,” Int. J. Innov. Res. Comput. Sci. Technol., vol. 8, no. 2, pp. 37–42, 2020, doi: 10.21276/ijircst.2020.8.2.5.
[3] S. Adamović, V. Miškovic, N. Maček, and M. Milosavljević, “An efficient novel approach for iris recognition based on stylometric features and machine learning techniques,” Futur. Gener. Comput. Syst., vol. 107, pp. 144–157, 2020, doi: 10.1016/j.future.2020.01.056.
[4] P. Patil and K. Vasanth, "Iris Recognition Using Local and Global Iris Image Moment Features," 2019 Innovations in Power and Advanced Computing Technologies (i-PACT), Vellore, India, 2019, pp. 1-5, doi: 10.1109/i-PACT44901.2019.8960219
[5] P. R. Nalla and A. Kumar, "Toward More Accurate Iris Recognition Using Cross-Spectral Matching," in IEEE Transactions on Image Processing, vol. 26, no. 1, pp. 208-221, Jan. 2017, doi: 10.1109/TIP.2016.2616281.
[6] K. Wang and A. Kumar, "Cross-Spectral Iris Recognition using CNN and Supervised Discrete Hashing," Pattern Recognition vol. 86 no. August, pp. 1–39, 2018, doi.org/10.1016/j.patcog.2018.08.010.
[7] M. Oktiana, T. Horiuchi, K. Hirai, K. Saddami, and F. Arnia, "Heliyon Cross-spectral iris recognition using phase-based matching and homomorphic filtering," Heliyon, vol. 6, no. April 2019, p. e03407, 2020, doi: 10.1016/j.heliyon.2020.e03407
[8] M. Mostofa, F. Taherkhani, J. Dawson and N. M. Nasrabadi, "Cross-Spectral Iris Matching Using Conditional Coupled GAN," 2020 IEEE International Joint Conference on Biometrics (IJCB), Houston, TX, USA, 2020, pp. 1-9, doi: 10.1109/IJCB48548.2020.9304929
[9] Vyas, R., Kanumuri, T. & Sheoran, G." Cross spectral iris recognition for surveillance-based applications." Multimed Tools Appl 78, 5681–5699 (2019),doi. org/10.1007/s11042-018-5689-y
[10] M. Oktiana et al., "Advances in Cross-Spectral Iris Recognition Using Integrated Gradientface-Based Normalization," in IEEE Access, vol. 7, pp. 130484-130494, 2019, doi 10.1109/ACCESS.2019.2939326.
[11] M. Oktiana, K. Saddami, F. Arnia, Y. Away, and K. Munadi, "Improved Cross-Spectral Iris Matching Using Multi-Scale Weberface and Gabor Local Binary Pattern," 2018 10th International Conference on Electronics, Computers and Artificial Intelligence (ECAI), Iasi, Romania, 2018, pp. 1-6, doi: 10.1109/ECAI.2018.8679097
[12] Vishwakarma, V. P., & Dalal, S. (2020). A novel approach for compensation of light variation effects with KELM classification for efficient face recognition. In Advances in VLSI, Communication, and Signal Processing: Select Proceedings of VCAS 2018 (pp. 1003-1012). Springer Singapore.
[13] Dalal, S., & Vishwakarma, V. P. (2020). A novel approach of face recognition using optimized adaptive illumination–Normalization and KELM. Arabian Journal for Science and Engineering, 45, 9977-9996.
[14] Chandrakala, M., & Devi, P. D. (2021). Two-stage classifier for face recognition using HOG features. Materials Today: Proceedings, 47, 5771-5775.
[15] Ghaffari, S., Soleimani, P., Li, K. F., & Capson, D. W. (2020). Analysis and comparison of FPGA-based histogram of oriented gradients implementations. IEEE Access, 8, 79920-79934.
[16] Mostafiz, R., Uddin, M. S., Alam, N. A., Hasan, M. M., & Rahman, M. M. (2021). MRI-based brain tumour detection using the fusion of histogram oriented gradients and neural features. Evolutionary Intelligence, 14, 1075-1087.
[17] Anowar, F., Sadaoui, S., & Selim, B. (2021). Conceptual and empirical comparison of dimensionality reduction algorithms (PCA, kpca, lda, mds, svd, lle, isomap, le, ica, t-sne). Computer Science Review, 40, 100378
[18] Choubey, D. K., Kumar, M., Shukla, V., Tripathi, S., & Dhandhania, V. K. (2020). Comparative analysis of classification methods with PCA and LDA for diabetes. Current diabetes reviews, 16(8), 833-850.
[19] Fabiyi, S. D., Murray, P., Zabalza, J., & Ren, J. (2021). Folded LDA: extending the linear discriminant analysis algorithm for feature extraction and data reduction in hyperspectral remote sensing. IEEE Journal of selected topics in applied earth observations and remote sensing, 14, 12312-12331.
[20]H. S. Hu and D. Z. Feng, “Minimum eigenvector collaborative representation discriminant projection for feature extraction,” Sensors (Switzerland), vol. 20, no. 17, pp. 1–20, 2020, doi: 10.3390/s20174778.

[21]J. Vasavi and M. Abirami, "A Qualitative Performance Comparison Of Supervised Machine Learning Algorithms For Iris Recognition," Eur. J. Mol. Clin. Med., vol. 07, no. 06, p. 2020, 2020.
[22] Berry, M. W., Mohamed, A., & Yap, B. W. (Eds.). (2019). Supervised and unsupervised learning for data science. Springer Nature.
[23] Saranya, T., Sridevi, S., Deisy, C., Chung, T. D., & Khan, M. A. (2020). Performance analysis of machine learning algorithms in intrusion detection system: A review. Procedia Computer Science, 171, 1251-1260.
[24] Dey, S., Wasif, S., Tonmoy, D. S., Sultana, S., Sarkar, J., & Dey, M. (2020, February). A comparative study of support vector machine and Naive Bayes classifier for sentiment analysis on Amazon product reviews. In 2020 International Conference on Contemporary Computing and Applications (IC3A) (pp. 217-220). IEEE.
[25] Parady, G., Ory, D., & Walker, J. (2021). The overreliance on statistical goodness-of-fit and under-reliance on model validation in discrete choice models: A review of validation practices in the transportation academic literature. Journal of Choice Modelling, 38, 100257.
[26] The Hong Kong Polytechnic University Cross-Spectral Iris Images Database, Aug.2018 [online] Available: http://www4.comp.polyu.edu.hk.